Tunable dual-wavelength actively *Q*-switched Er/Yb double-clad fiber laser

2014 Laser Phys. Lett. 11 015102

(http://iopscience.iop.org/1612-202X/11/1/015102)

IOP Publishing | Astro Ltd Laser Physics Letters

Laser Phys. Lett. **11** (2014) 015102 (5pp) doi:10.1088/1612-2011/11/1/015102

Letter

Tunable dual-wavelength actively Q-switched Er/Yb double-clad fiber laser

M Durán-Sánchez[1], E A Kuzin[2], O Pottiez[3], B Ibarra-Escamilla[2], A González-García[2,4], F Maya-Ordoñez[2], R I Álvarez-Tamayo[1] and A Flores-Rosas[5]

[1] Universidad Tecnológica de Puebla, Mecatrónica, Antiguo Camino a la Resurrección 1002-A, Parque Industrial Puebla, 72300 Puebla, Puebla, Mexico
[2] Instituto Nacional de Astrofísica, Óptica y Electrónica, Optics Department, Luis Enrique Erro 1, 72000 Puebla, Puebla, Mexico
[3] Centro de Investigaciones en Óptica, Fiber Optics Department, Lomas del Bosque 115, 37150 León, Guanajuato, Mexico
[4] Instituto Tecnológico Superior de Guanajuato Carretera Estatal Guanajuato-Puentecillas, km 10.5, Guanajuato, 36262 Gto, Mexico
[5] Universidad de Guanajuato, Campus Irapuato-Salamanca, Carretera Salamanca-Valle de Santiago km 3.5+1.8, Salamanca, Gto, Mexico

E-mail: maratonista80@hotmail.com

Received 31 July 2013, in final form 26 October 2013
Accepted for publication 28 October 2013
Published 15 November 2013

Abstract

We demonstrate experimentally a dual-wavelength tunable actively Q-switched fiber laser using 3 m of Er^{3+}/Yb^{3+} co-doped fiber as the gain medium. For wavelength tuning we used a tunable Hi-Bi FBG having two reflection wavelengths separated by 0.4 nm. The laser emits a dual-wavelength signal that is tunable in a range of 11.8 nm. Laser operation can be switched between single and double wavelength emission. The laser operates at repetition rates from 30 to 110 kHz with pulse durations of 280 ns and pulse energies near 0.5 μJ.

(Some figures may appear in colour only in the online journal)

1. Introduction

Multi-wavelength Q-switched fiber lasers have generated great interest because of their potential application as a source in different areas, such as remote sensing, biomedicine, laser processing, microwave optics, telecommunications and terahertz generation. Several experimental setups have been proposed to generate Q-switched laser pulses, including passive and active approaches. In passively Q-switched lasers, different techniques have been proposed, including the development of saturable absorbers using short carbon nanotubes [1, 2] and graphene [3, 4], among others [5, 6]. Moreover, recent investigations on active Q-switched fiber lasers have focused on novel optical modulation devices [7–9] and laser geometry designs [10]. The advantages of actively Q-switched fiber lasers include improved stability, higher energy pulses, or lower insertion loss, with disadvantages related to alignment problems caused by the bulk architecture and increased complexity of the cavity [17–20].

Nowadays, the potential applications of Q-switched fiber lasers suggest that additional characteristics such as wavelength tuning would be attractive. Several designs of both active and passive tunable Q-switched fiber lasers operating at a single wavelength have been reported, where fiber Bragg gratings [2], a dielectric interference filter [3] or tunable band-pass filters [4] are the most common tuning mechanisms.

Recently, the interest in dual-wavelength laser generation has increased. For dual-wavelength Q-switched pulsed fiber lasers both passive [11–14] and active [15–17] approaches

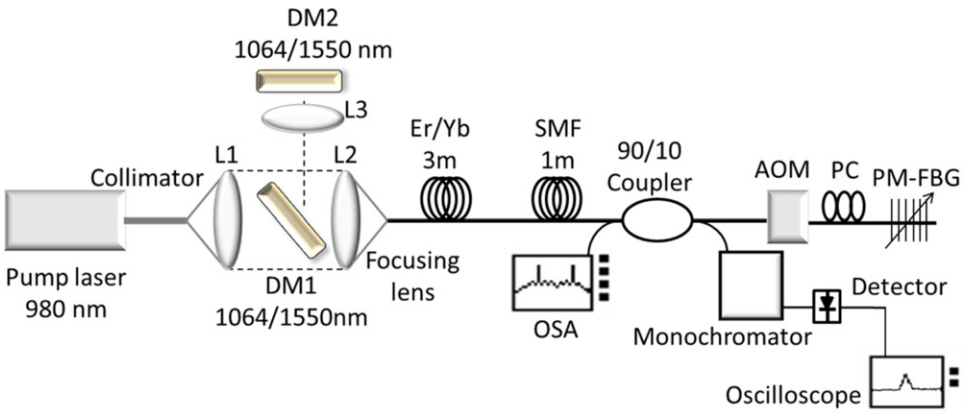

Figure 1. Configuration setup for the tunable double-wavelength fiber laser.

has been reported. In the case of passive *Q*-switched fiber lasers Liu *et al* [14] reported a pulsed erbium doped fiber laser based on a single-wall carbon nanotube saturable absorber, with a pulse energy around 0.5 nJ and two laser lines at 1532 and 1558 nm. Wang *et al* [12] demonstrated a switchable dual-wavelength pulsed fiber laser using a graphene saturable absorber with two different laser lines, reaching a pulse energy up to 70 nJ. On the other hand, in the frame of active *Q*-switching designs, Sharma *et al* [15] reported a complex ring cavity configuration with a discrete tuning range of 2.2 nm in wavelength spacing. Li *et al* [17] reported a diode-cladding-pumped dual-wavelength *Q*-switch Ho^{3+} doped fluoride cascaded free-space fiber laser operating in the mid-infrared region.

Double-clad rare-earth-doped fibers are attractive for fiber amplifiers and laser system designs due to their high power, high beam quality, and heat dissipation advantages [5, 18–20]. The use of such fibers in single-wavelength *Q*-switched lasers has been reported. For example, Loroche *et al* [5] reported an Er^{3+}/Yb^{3+} double-clad passive linear cavity *Q*-switched tunable fiber laser. González-García *et al* [18] experimentally demonstrated active *Q*-switched fiber laser operation using an Er^{3+}/Yb^{3+} doped double-clad fiber and an acousto-optic modulator in a free-space design.

In this letter we report a *Q*-switched dual-wavelength tunable Er^{3+}/Yb^{3+} fiber laser using a polarization-maintaining fiber Bragg grating (PM-FBG) in a Fabry–Perot configuration. The PM-FBG was mechanically compressed/stretched, allowing a total wavelength tuning range of ∼11.8 nm. The pulse energy was approximately 0.5 μJ with a pulse duration of 280 ns (FWHM).

2. Experimental setup

The schematic diagram of the laser under study is shown in figure 1. The optical setup is a combination of two optical sub-systems operating at different wavelengths, one of them is the pump system at 976 nm and the other one is the laser system at 1549 nm. The pump was introduced into the cavity by a lens L1, a dichroic mirror DM1, and a lens L2. The maximum power of a pump laser diode was 50 W. However the maximum power used in experiments was 2 W to avoid damage to the acousto-optical modulator with a maximal permitted average power of 1 W. The dichroic mirror (DM2) and fiber Bragg grating written in polarization-maintaining fiber (PM-FBG) are used as cavity end mirrors. Wavelength tuning of the PM-FBG is performed by applying axial compression or stretching using a micrometric screw. The maximum compression applied is about 80 μm causing a maximum wavelength displacement of 8.12 nm. The corresponding wavelength shift rate is about 1.1 nm/10 μm. The maximum stretch is 40 μm, causing a wavelength shift of 3.67 nm, which corresponds to a rate of 0.91 nm/10 μm. The total laser wavelength shift is ∼11.8 nm with an average rate of approximately 0.98 nm/10 μm. A polarization controller (PC) inserted into the cavity allows switching between single- and dual-wavelength modes of operation. The gain medium of the laser is a 3-m length of Er^{3+}/Yb^{3+} co-doped, double-clad fiber, which has a core diameter of 7 μm, an inner cladding diameter of 130 μm, and an outer cladding diameter of 245 μm. The numerical aperture for the signal is 0.17 and the inner to outer cladding NA is 0.46. The end of the Er^{3+}/Yb^{3+} doped fiber was spliced to a 1-m length of Corning SMF-28 fiber, in order to attenuate the residual pump and also to reduce the 1064 nm signal due to the ytterbium emission. Two aspheric lenses, L1 of 18 mm focal length and L2 of 8 mm focal length, were used to focus the pump and signal into the Er^{3+}/Yb^{3+} fiber.

Lens L3 with a focal length of 150 mm was used in the system to increase the stability of the laser emission. The experimental setup includes two short-wave pass (SWP) dichroic mirrors DM1 and DM2 with high reflectivity (>99.5%) at 1550 nm and high transmission (>90%) at 1064 nm, at 45° and 0° incidence angles, respectively. The Er^{3+}/Yb^{3+} fiber was pumped by a high-power laser diode (JOLD-30-FC-12-976). The output fiber of the laser diode is characterized by a core diameter of 200 μm and a numerical aperture of 0.22. Two ports of the 90/10 coupler were used to measure simultaneously the spectrum with an optical spectrum analyzer (OSA) and the pulse shapes at different wavelengths using a monochromator and a fast photodetector. The OSA has a resolution of 0.01 nm; the monochromator has a resolution of 0.2 nm.

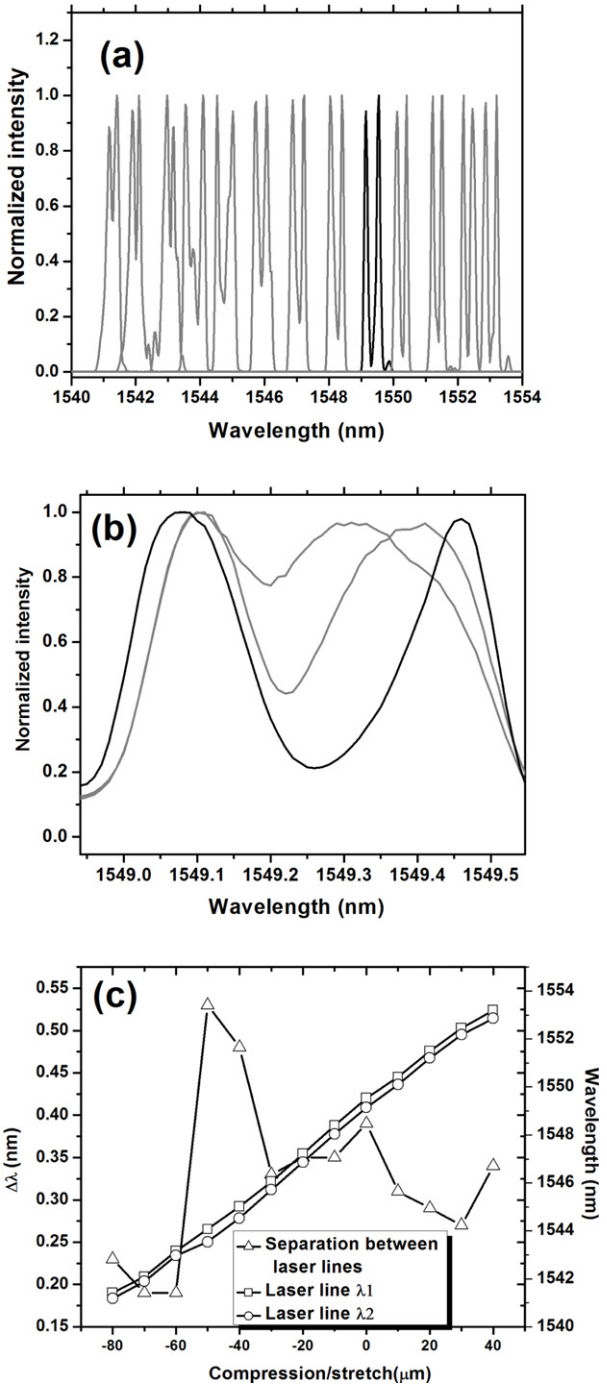

Figure 2. Tunable dual-wavelength Q-switched fiber laser spectra.

3. Experimental results and discussion

Figure 2(a) shows the output spectra measured by the OSA for 12 values of stretch/compression of the PM-FBG. Two emission laser lines at 1549.14 and 1549.54 nm were measured without stretch/compression (solid black line). For each compression/stretch of the PM-FBG we adjusted the PC to obtain dual-wavelength operation. As can be seen, the separation between the two generated laser lines varies for each wavelength tuning. This behavior is attributable to

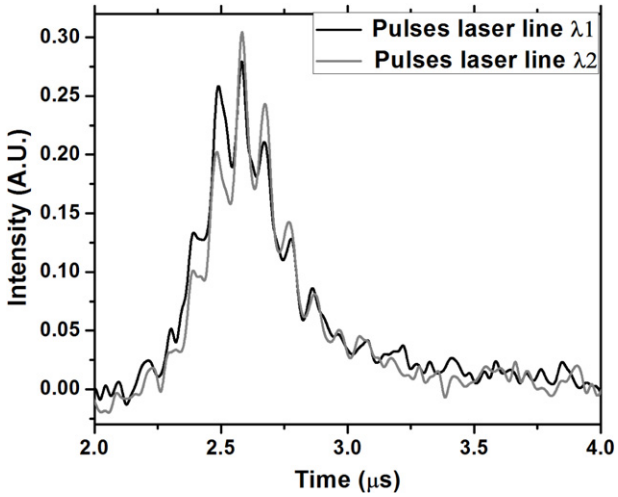

Figure 3. Profile of the pulses at $\lambda 1 = 1549.17$ nm and $\lambda 2 = 1549.54$ nm.

the PC adjustment applied to obtain two simultaneous laser lines. The separation between lines can indeed be modified by PC adjustment. Figure 2(b) shows the spectra for the same tuning of the PM-FBG at three different adjustments of the PC. Switching between laser lines can also be performed by adjustment of the PC. Figure 2(c) shows the laser lines separation for the same 12 values of stretch/compression as in figure 2(a) (point triangles line). As can be seen, the maximum and minimum separations are around 0.52 nm and 0.19 nm respectively. On the right side scale is presented the central wavelength of each laser line for each value of stretch/compression. The tuning range is ∼11.8 nm for a compression/stretch range of 120 μm, which corresponds to an average rate of approximately 0.95 nm/10 μm.

Figure 3 shows the pulses filtered by the monochromator with a resolution of 0.2 nm at 1549.17 nm (black line) and 1549.54 nm (gray line), which correspond to the two wavelengths shown in figure 2(a) (solid black line). The pulse repetition rate is 100 kHz. The monochromator scanning is used to verify the presence of pulses for each laser line, corresponding to dual-wavelength generation. As can be seen, the pulses for both laser lines have similar powers and shapes.

The time shift between the leading edge of the electrical pulse applied to the modulator and the leading edge of the laser pulse is 2.2 μs. This shift depends on the wavelength tuning of the laser. Figure 4(a) shows examples of the pulse waveforms for different wavelength tunings together with the leading edge of the pulse applied to the modulator. We can see that the displacement depends on the stretch/compression value. The dependence of the temporal displacement on the stretch/compression is shown in figure 4(b). It appears that for shorter wavelengths the time displacement is smaller than for longer wavelengths. Beyond $\Delta\lambda = -6$ nm, the temporal position of the pulses begin to stabilize around a minimal value of 1.6 μs.

The average output power in dual-wavelength operation (at 1549.17 and 1549.54 nm) as a function of the repetition rate, measured over a range from 20 to 120 kHz with a pump

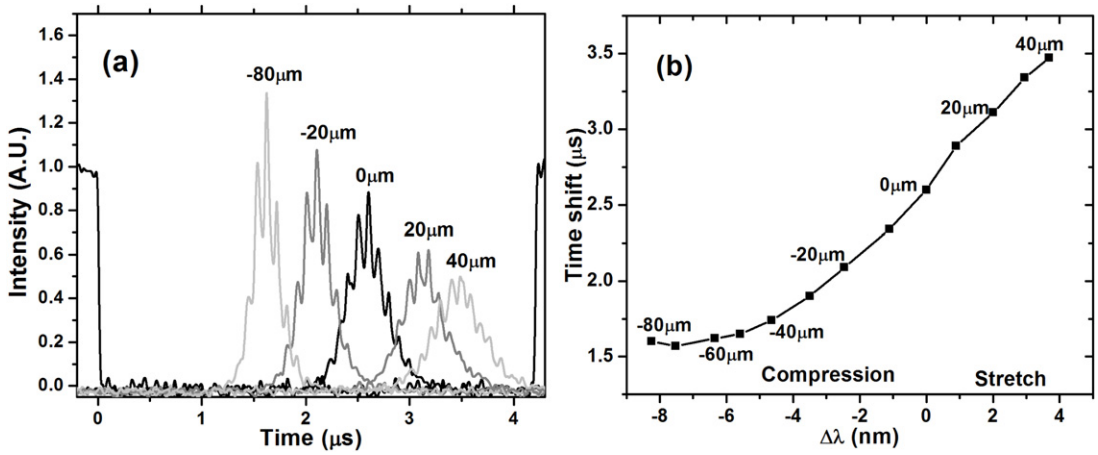

Figure 4. Pulse delay versus wavelength displacement. Labels in the figures refer to stretch/compression values.

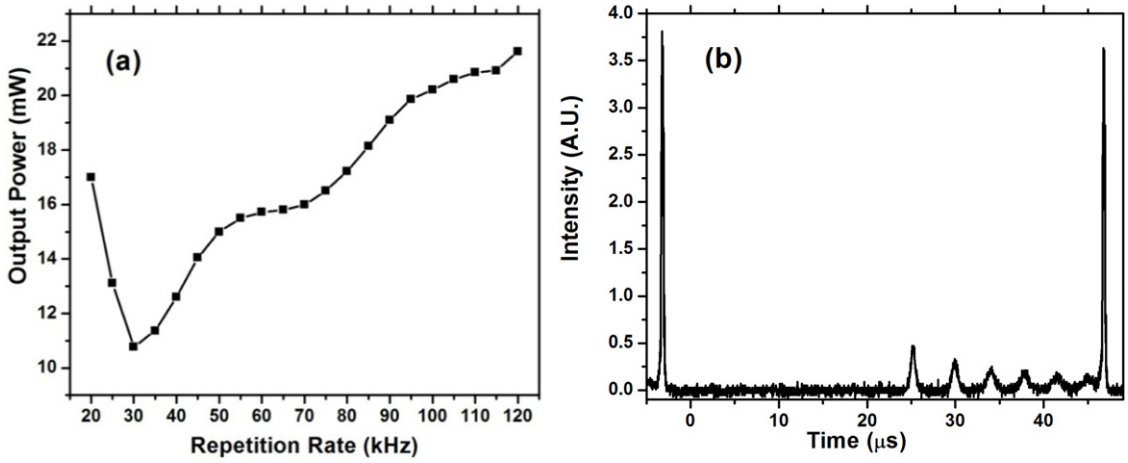

Figure 5. Output power as a function of repetition rate (a) and typical oscilloscope trace of optical pulses at a 20 kHz repetition rate (b).

power of 1.5 W, is shown in figure 5(a). As can be seen, overall the average power increases with repetition frequency. An exception occurs below 30 kHz. In this case, during the long time between modulation pulses, the amplification of the doped fiber increases to a level sufficient to produce spurious generation. This happens even when the modulator is closed. This spurious generation can be observed in figure 5(b) when the laser operates at 20 kHz. Between the two large generated pulses we can observe five small pulses due to spurious oscillation.

Figure 6 shows the pulse duration and the pulse energy as a function of the repetition rate for a fixed wavelength adjustment corresponding to the generation of laser lines at 1549.14 and 1549.54 nm. For these measurements, the pump power was increased to 2 W. As is shown, the pulse energy decreases with increasing repetition rate due to the decrease of the energy stored in the doped fiber as the time between consecutive pulses shortens. On the other hand, as can be seen, the pulse duration increases as the repetition rate increases. At a repetition rate of 100 kHz, the Q-switched laser generates pulses with a duration of 0.55 μs and an energy of 0.22 μJ with an average output power of 20 mW measured at the 10% coupler output.

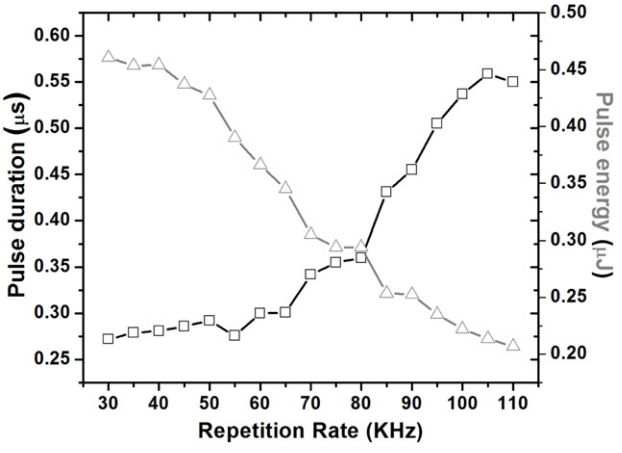

Figure 6. Pulse duration (square points curve) and pulse energy (triangle points curve) as a function of the repetition rate of the tunable actively Q-switched laser.

4. Conclusions

We have demonstrated experimentally a dual-wavelength and tunable actively Q-switched fiber laser with an Er^{3+}/Yb^{3+}

double cladding fiber as the active medium. A PM-FBG is used as the tunable spectral filter. Double- or single-wavelength operation is determined by adjustment of a PC, which also allows control of the separation between the two lasing lines. The laser operates at repetition rates from 30 to 110 kHz with pulse durations of 280 ns and pulse energies near 0.5 μJ. For lower pulse repetition rates a spurious generation appears between pulses. On the other hand, for pulse repetition rates over 110 kHz the pulse generation begins to decline because the limit of the AOM window is reached.

Acknowledgment

This work was supported by CONACYT project CB2010-151434.

References

[1] Dong B, Hao J, Hu J and Liaw C-Y 2011 *Opt. Fiber Technol.* **17** 105
[2] Dong B, Liaw C-Y, Hao J and Hu J 2010 *Appl. Opt.* **49** 5989
[3] Popa D, Sun Z, Hassan T, Torrisi F, Wang F and Ferrari A C 2011 *Appl. Phys. Lett.* **98** 0731106
[4] Zhou D-P, Wei L and Liu W-K 2012 *Appl. Opt.* **51** 2554
[5] Loroche M, Chardon A M, Nilsson J, Shepherd D P and Clarkson W A 2002 *Opt. Lett.* **27** 1980
[6] Pérez-Millán P, Díez A, Cruz J L and Andrés M V 2009 *Opt. Commun.* **282** 621
[7] Delgado-Pinar M, Zalvidea D, Diez A, Pérez-Millán P and Andrés M V 2006 *Opt. Express* **14** 1106
[8] Anderson T V, Pérez-Millán P, Keiding S R, Agger S, Duchowicz R and Andrés M V 2006 *Opt. Commun.* **260** 251
[9] Cuadrado-Laborde C, Díez A, Cruz J L and Andrés M V 2009 *Opt. Lett.* **34** 2709
[10] Escalante-Zarate L, Barmenkov Y O, Kolpakov S A, Cruz J L and Andrés M V 2012 *Opt. Express* **20** 4397
[11] Luo Z, Zhou M, Weng J, Huang G, Xu H, Ye C and Cai Z 2010 *Opt. Lett.* **35** 3709
[12] Wang Z T, Chen Y, Zhao C J, Zhang H and Wen S C 2012 *IEEE Photon. J.* **4** 869
[13] Dong B, Hu J, Yu C and Hao J 2012 *Opt. Commun.* **285** 3864
[14] Liu L, Zheng Z, Zhao X, Sun S, Bian Y, Su Y, Liu J and Zhu J 2013 *Opt. Commun.* **294** 267
[15] Sharma U, Kim C-S and Kang J U 2004 *IEEE Photon. Technol. Lett.* **16** 1277
[16] Barmenkov Y O, Kir'yanov A V, Zalvidea D, Torres-Peiró S, Cruz J L and Andrés M V 2007 *IEEE Photon. Technol. Lett.* **19** 480
[17] Li J, Hu T and Jackson S D 2012 *Opt. Lett.* **37** 2208
[18] González-García A, Ibarra Escamilla B, Pottiez O, Kuzin E A, Maya-Ordoñez F, Duran-Sánchez M, Deng C, Haus J W and Powers P E 2013 *Opt. Laser Technol.* **48** 182
[19] Liu C, Ye C, Luo Z, Cheng H, Wu D, Zheng Y, Liu Z and Qu B 2013 *Opt. Express* **21** 204
[20] Huang J Y, Huang S C, Chang H L, Su K W, Chen Y F and Huang K F 2008 *Opt. Express* **16** 3002